

# Polarization and ellipticity of high-order harmonics from aligned molecules generated by linearly polarized intense laser pulses

Anh-Thu Le,<sup>1</sup> R. R. Lucchese,<sup>2</sup> and C. D. Lin<sup>1</sup>

<sup>1</sup>*Department of Physics, Cardwell Hall, Kansas State University, Manhattan, KS 66506, USA*

<sup>2</sup>*Department of Chemistry, Texas A&M University, College Station, Texas 77843-3255, USA*

(Dated: November 23, 2018)

We present theoretical calculations for polarization and ellipticity of high-order harmonics from aligned N<sub>2</sub>, CO<sub>2</sub>, and O<sub>2</sub> molecules generated by linearly polarized lasers. Within the rescattering model, the two polarization amplitudes of the harmonics are determined by the photo-recombination amplitudes for photons emitted parallel and perpendicular to the direction of the *same* returning electron wave packet. Our results show clear species-dependent polarization states, in excellent agreement with experiments. We further note that the measured polarization ellipse of the harmonic furnishes the needed parameters for a “complete” experiment in molecules.

PACS numbers: 33.80.Eh, 42.65.Ky

High-order harmonic generation (HHG) is one of the most important nonlinear processes that occur when atoms or molecules are placed in an intense laser field [1]. Today these high harmonics are used as convenient laboratory XUV or soft X-ray light sources, as well as the sources of single attosecond pulses or attosecond pulse trains [2–4]. High harmonics are emitted when laser-induced continuum electrons recombine with the target ions. Since photo-recombination is a time-reversed process of photoionization (PI), study of HHG from molecular targets offers alternative means for probing molecular structure that have been traditionally carried out using PI at synchrotron radiation facilities. Gaseous molecules can be given a periodic transient alignment by a weak short laser pulse [5]. By studying HHG generated from such aligned molecules, information such as molecular frame photoelectron angular distributions (MFPAD) for PI from valence orbitals of molecules can be inferred. The goal of a “complete experiment” is to determine amplitudes and phases of all dipole matrix elements. For linear molecules, this may be achieved if measurements of MFPAD are carried out using elliptically polarized lights [6, 7]. For photo-recombination, this means that one may obtain equivalent information by examining the elliptical polarization of HHG from aligned molecules.

Clearly if the gas is isotropically distributed, as for atomic or unaligned molecular targets, due to the symmetry the emitted harmonics are polarized parallel to the polarization of the driving linearly polarized laser. For aligned molecules, a harmonic component perpendicular to the laser polarization is expected to be present in general [8]. This requires that experiments be carried out with a good level of molecular alignment in order to observe a significant amount of the perpendicular harmonic component. It is therefore not surprising that polarization measurements for emitted harmonics were reported only very recently [9–13]. All these experiments were carried out within the pump-probe scheme, where a relatively weak, short laser pulse is used to impulsively

align molecules along its polarization direction, and after some delay time, a second laser pulse is used to generate high-order harmonics. We note that the commonly used strong-field approximation (SFA) cannot be employed to interpret such experiments since it predicts little or no ellipticity for emitted harmonics [9, 14].

In this Letter we report theoretical results for polarization and ellipticity of HHG from aligned N<sub>2</sub>, O<sub>2</sub>, and CO<sub>2</sub> molecules. Our results show very good agreement with experimental measurements [9, 10, 13] for harmonic orientation angles and the reported large ellipticity for N<sub>2</sub> [13]. The calculations were carried out using the quantitative rescattering theory (QRS) [15–19] where the complex induced dipole responsible for harmonic emission is represented as a product of a returning electron wave packet and the *laser-free* photo-recombination transition dipole,

$$D_{\parallel,\perp}(\omega, \vartheta) = W(E_k, \vartheta) d_{\parallel,\perp}(\omega, \vartheta). \quad (1)$$

Here  $\vartheta$  is the angle between the molecular axis and the (probe) laser polarization direction,  $E_k$  is the “incident” energy of the returning electron, and  $\omega = I_p + E_k$  is the emitted photon energy, with  $I_p$  being the ionization potential. The returning electron can recombine with the parent ion to emit a photon with polarization in the parallel or perpendicular direction to its motion, resulting in the two polarization components of the emitted harmonics. Both of these complex transition dipoles  $d_{\parallel,\perp}$  are obtained from state-of-the-art molecular photoionization code [20, 21] for each fixed-in-space molecule. Note that we only need to consider the harmonic components on the plane perpendicular to the propagation direction of the driving laser, since only the harmonic emission propagating along this direction can be efficiently phase matched. As for the returning electron wave packet, we extract it from the SFA [16]. Eq. (1) thus shows that the amplitude and phase of the transition dipoles can be probed by studying HHG.

To compare with experiments, induced dipoles

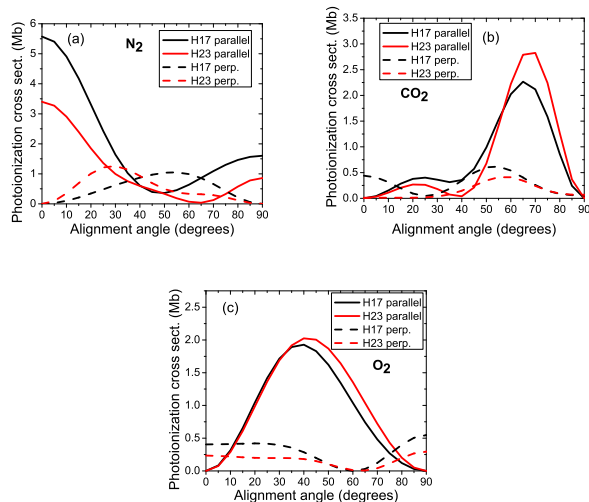


FIG. 1: (Color online) Fixed-in-space molecular photoionization differential cross sections, corresponding to the parallel and perpendicular components of emitted harmonics H17 and H23 for  $N_2$  (a),  $CO_2$  (b), and  $O_2$  (c).

$D_{\parallel,\perp}(\omega, \vartheta)$  from the fixed-in-space molecules are coherently convoluted with the molecular alignment distributions [8, 16, 22]. We note that this alignment “phase-matching” tends to favor the parallel component. In our simulations, the alignment distribution is obtained from numerical solution of the time-dependent Schrödinger equation within the linear rotor model for each molecular species [5, 16]. We use a 120 fs pump laser pulse with an intensity of  $3 \times 10^{13}$  W/cm<sup>2</sup>, and a 30 fs probe laser pulse with an intensity of  $2 \times 10^{14}$  W/cm<sup>2</sup>. Both pump and probe lasers are of 800 nm wavelength. The rotational temperature is assumed to be 100 K. These parameters were chosen to closely match the experimental conditions of Zhou *et al* [13]. We vary the angle between pump and probe polarizations and use the half-revival time delay for  $N_2$  and  $O_2$ , and 3/4-revival for  $CO_2$ .

To understand the experimental measurements, we show in Fig. 1 fixed-in-space PI differential cross sections for the three species, corresponding to the parallel and perpendicular components of emitted harmonics H17 and H23. Note that these cross sections are proportional to  $|d_{\parallel}|^2$  and  $|d_{\perp}|^2$ , respectively. In general, the perpendicular components are smaller than the parallel components for all three targets. Due to symmetry, the perpendicular harmonic component will vanish after averaging over the alignment distribution if the angle between pump and probe polarizations  $\theta$  is  $0^\circ$  or  $90^\circ$  (see Fig. 2 below). From Fig. 1 we note that at intermediate angles the cross section for the perpendicular component is quite comparable to the parallel one for  $N_2$  and  $CO_2$ . For  $O_2$  the perpendicular is always much smaller than the parallel one. Therefore one can expect a small intensity ratio between perpendicular and parallel components for  $O_2$ , but

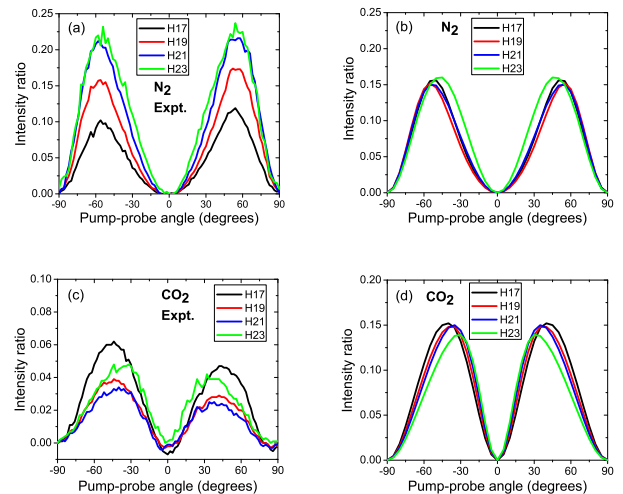


FIG. 2: (Color online) Experimental (left panels) and theoretical (right panels) intensity ratios between perpendicular and parallel component of harmonic fields, as a function of alignment angle between pump and probe polarization directions, for  $N_2$  (top panels) and  $CO_2$  (bottom panels). Experimental results are taken from Zhou *et al* [13].

a larger ratio for both  $N_2$  and  $CO_2$ .

Next we show in Fig. 2(b) and 2(d) theoretical intensity ratio  $\frac{I_{\perp}}{I_{\parallel}}$  between perpendicular and parallel components for harmonic orders from H17 to H23, as a function of alignment angle  $\theta$  between pump and probe polarizations. Experimental results by Zhou *et al* [13] are shown in Fig. 2(a) and 2(c) for comparison. For  $N_2$ , the theoretical intensity ratio reaches 0.16 at the peak near  $55^\circ$  for all the harmonics from H17 to H23 [Fig. 2(b)]. The measurement [13] shows a very similar shape with peaks near  $55^\circ$  as well, but the magnitude increasing with harmonic orders from 0.1 to 0.22. For  $CO_2$  [Fig. 2(d)], the shape of the intensity ratio from theory changes slightly, with the peak now at about  $40^\circ$ . This is also in good agreement with experiment. As for the magnitude, the theoretical intensity ratio is about a factor of three larger than in the experiment. This discrepancy could be partly due to the fact that near the minimum of the parallel component [see Fig. 1(b)] the theoretical transition dipole is not accurate enough or that inner molecular orbitals may contribute [23, 24]. For  $O_2$ , we found that the intensity ratio is very small, as expected, with the biggest intensity ratio of about 1% near  $35^\circ$ . We comment that for all three targets, the ratio goes to zero if pump and probe polarizations are parallel or perpendicular. As stated earlier, this is expected from symmetry consideration.

Let  $\delta$  be the phase difference between perpendicular and parallel components of the harmonic field and  $\tan(\gamma) = \sqrt{\frac{I_{\perp}}{I_{\parallel}}}$ . As  $\delta \neq 0$  or  $\pi$  in general, the emitted harmonic is elliptically polarized. To characterize the po-

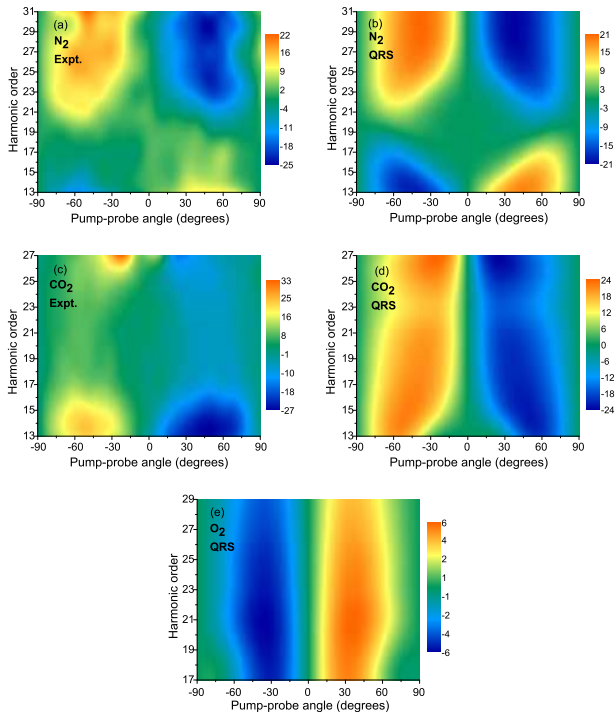


FIG. 3: (Color online) Experimental (left panels) and theoretical (right panels) orientation angle  $\phi$  (in degrees) as a function of alignment angle between pump and probe polarization directions and harmonic order for  $N_2$  (top panels),  $CO_2$  (middle panels). Experimental results are taken from Zhou *et al* [13]. Theoretical result for  $O_2$  is also showed (e).

larization ellipse, we define [25] the orientation angle  $\phi$  of the ellipse and the ellipticity  $\epsilon = \tan(\chi)$  by

$$\tan(2\phi) = \tan(2\gamma) \cos(\delta), \quad (2)$$

$$\sin(2\chi) = \sin(2\gamma) \sin(\delta). \quad (3)$$

Our results for the orientation angle  $\phi$  are shown in Fig. 3(b) and 3(d), as a function of alignment angle between pump and probe polarizations and harmonic order. Experimental results by Zhou *et al* [13] are also shown (left panels) for comparison. The theoretical data are anti-symmetric with respect to the sign change in the pump-probe angle  $\theta$ , so in the following we just focus on the positive  $\theta$ . The experimental data are less symmetric. Here the positive (or negative) angle corresponds to the case when the major axis of the ellipse rotates in the same (or opposite) direction as the molecular axis.

The most noticeable feature for  $N_2$  is the sign change in the orientation angle as a function of harmonic order near H19. The orientation angle of about  $20^\circ$  at H13, decreases smoothly with harmonic order, and reaches  $-20^\circ$  at H29. This is in excellent agreements with the measurements by Zhou *et al*, shown in Fig. 3(a), as well as with Levesque *et al* [9]. Zhou *et al* [13] found that the sign of the orientation angle changes near H19, while Levesque

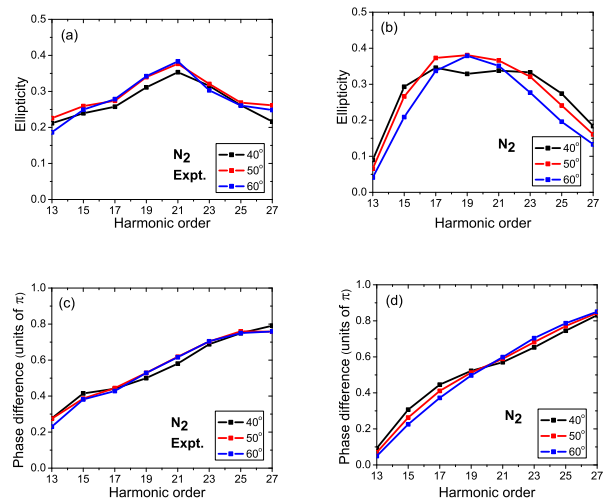


FIG. 4: (Color online) Experimental (left panels) and theoretical (right panels) ellipticity (top panels) and phase difference (bottom panels) between the two polarization components from  $N_2$  for angles between pump and probe polarizations  $\theta = 40^\circ, 50^\circ, 60^\circ$ . Experimental results are taken from Zhou *et al* [13].

*et al* [9] found the change near H21, independent of the pump-probe polarization angle. We comment that calculations based on the SFA do not lead to a satisfactory agreement with experiments [9]. For  $CO_2$ , the theoretical orientation angles are negative (for positive  $\theta$ ) for all the considered harmonics. This is in good agreements with Zhou *et al*, shown in Fig. 3(c), and Levesque *et al* [9]. For  $O_2$ , on the other hand, the orientation angle remains positive for the harmonic range shown in the figure. Its magnitude is also much smaller, reaching about  $6^\circ$  near H19-H21 for  $\theta \sim 30^\circ - 40^\circ$ . This behavior agrees well with Levesque *et al* [9]. Again, these small orientation angles are due to the small intensity ratios, which in turn is related to the smallness of the PI cross sections for the perpendicular component, as compared to the parallel component, for intermediate angles in  $O_2$  [see Fig. 1(c)].

We also compare ellipticity  $\epsilon$  and phase difference  $\delta$  vs harmonics order at fixed pump and probe angles  $\theta = 40^\circ, 50^\circ$ , and  $60^\circ$ . Fig. 4 shows that the theoretical results for  $N_2$  are in good agreement with the experimental data of Zhou *et al* [13]. In particular, the theory predicts a large ellipticity up to  $\epsilon \approx 0.4$  near H21, in agreement with experiment. We comment that a recent calculation based on an extended stationary-phase SFA by Etches *et al* [14] showed very weak ellipticity of about 0.02 only. The phase difference, shown in Fig. 4(d), increases nearly linearly with harmonic order, from  $0.1\pi$  at H13 to  $0.8\pi$  at H27, but is nearly independent of alignment angle. Note that the phase difference is nearly  $\pi/2$  at H19. This is exactly the harmonic order, where the orientation angle changes its sign, see Eq. (2) and Fig. 3(b). This behav-

ior is in excellent agreement with experiment shown in Fig. 4(c). For CO<sub>2</sub> the ellipticity from the QRS is slightly smaller than that of N<sub>2</sub>, while the measurements by Zhou *et al* showed a value of less than 0.1. This discrepancy is consistent with the larger errors we found for the CO<sub>2</sub> intensity ratio, but the reason remains largely unclear at this moment. We further note that the calculation for CO<sub>2</sub> by Smirnova *et al* [23] showed an ellipticity of 0.1 at H29, which increases up to about 0.4 at harmonics H37-H43. In their simulation, contributions from two lower molecular orbitals were also included. For completeness we note that the QRS predicts an ellipticity for O<sub>2</sub> of less than 5% under the same experimental conditions.

In general, experimental HHG spectra include the effect of macroscopic propagation in the medium [26]. However, under typical experimental conditions, we can show that macroscopic propagation will affect both harmonic components in the same way. Indeed, the propagation equation for each harmonic component  $E_a$  (with  $a = \parallel$  or  $\perp$ ) can be written under the paraxial approximation as [26, 27]

$$\nabla_{\perp}^2 E_a(r, z, \omega, \theta) - \frac{2i\omega}{c} \frac{\partial E_a(r, z, \omega, \theta)}{\partial z} \propto \langle D_a(r, z, \omega) \rangle_{\theta}, \quad (4)$$

where  $\langle D_{\parallel, \perp}(r, z, \omega) \rangle_{\theta}$  is the nonlinear polarization, averaged over the molecular alignment distribution for a fixed pump-probe angle  $\theta$ . Here we assume that absorption and free-electron dispersion are negligible. In a typical gas jet experiment, the aligning laser is much less intense and more loosely focused than the probe laser. Therefore we can assume that the aligning laser is uniform in the gas jet, which is typically of about 1 mm thick. We found that for a fixed  $\{\omega, \theta\}$  the intensity ratio and phase difference between the two components  $\langle D_{\parallel}(\omega) \rangle_{\theta}$  and  $\langle D_{\perp}(\omega) \rangle_{\theta}$  change less than 10% as probe laser intensity changes from  $1.5 \times 10^{14}$  to  $2.5 \times 10^{14}$  W/cm<sup>2</sup>. In other words, the ratio  $R = |\langle D_{\perp} \rangle / \langle D_{\parallel} \rangle|$  and phase difference are nearly independent of the spatial coordinates  $\{r, z\}$  in the gas jet. From Eq. (4), it follows that the ratio  $|E_{\perp}/E_{\parallel}| = R$ . The same arguments also hold for the phase difference between  $E_{\perp}$  and  $E_{\parallel}$ . This implies that the results presented in this paper should be nearly unchanged even if the macroscopic propagation is carried out. Our results are still dependent on the degree of molecular alignment, which is controlled by the pump pulse. Therefore polarization resolved HHG measurements allow us to directly extract single-molecule features (up to averaging over the alignment distribution) without much influence of the details of the macroscopic phase-matching conditions.

In conclusion, we have shown that the quantitative rescattering theory can be extended to calculate polarization and ellipticity of high-order harmonics from aligned molecules in intense laser fields. Theoretical results are compared to experimental measurements side by side and good agreement has been found. The interaction of light

with molecules is governed by the dipole transition matrix elements. This dipole interaction has been traditionally probed using photoionization, but can similarly be probed by studying HHG. While photoionization has the advantage of achieving higher energy resolution to reveal many-electron dynamics, HHG has the advantage of surveying a broader photon energy range coherently in one single experiment, thus revealing the global property of the molecule. Since the phases of the harmonics can be conveniently measured experimentally, HHG also has the advantage of revealing directly the phases of the transition dipoles.

We thank X. Zhou, M. Murnane, and H. Kapteyn for providing us with their experimental data and the stimulating discussions. This work was supported in part by the Chemical Sciences, Geosciences and Biosciences Division, Office of Basic Energy Sciences, Office of Science, U. S. Department of Energy. RRL also acknowledges the support of the Welch Foundation (Houston, TX) under grant A-1020.

- 
- [1] F. Krausz and M. Ivanov, *Rev. Mod. Phys.* **81**, 163 (2009).
  - [2] M. Hentschel *et al.*, *Nature* **414**, 509 (2001).
  - [3] G. Sansone *et al.*, *Science* **314**, 443 (2006).
  - [4] T. Remetter *et al.*, *Nature Phys.* **2**, 323 (2006).
  - [5] H. Stapelfeldt and T. Seideman, *Rev. Mod. Phys.* **75**, 543 (2003).
  - [6] S. Motoki *et al.*, *J. Phys. B* **35** 3801 (2002).
  - [7] M. Lebeck *et al.* *J. Chem. Phys.* **118**, 9653 (2003).
  - [8] M. Lein *et al.*, *J. Mod. Optics* **52**, 465 (2005).
  - [9] J. Levesque *et al.*, *Phys. Rev. Lett.* **98**, 183903 (2007).
  - [10] Y. Mairesse *et al.*, *J. Mod. Optics* **55**, 2591 (2008).
  - [11] Y. Mairesse *et al.*, *New J. Phys.* **10**, 025028 (2008).
  - [12] G. H. Lee *et al.*, *Opt. Lett.* **33**, 2083 (2008).
  - [13] X. Zhou *et al.*, *Phys. Rev. Lett.* **102**, 073902 (2009).
  - [14] A. Etches, C. B. Madsen, and L. B. Madsen, *Phys. Rev. A* **81**, 013409 (2010).
  - [15] T. Morishita *et al.*, *Phys. Rev. Lett.* **100**, 013903 (2008).
  - [16] A. T. Le *et al.*, *Phys. Rev. A* **80**, 013401 (2009).
  - [17] A. T. Le *et al.*, *Phys. Rev. A* **78**, 023814 (2008).
  - [18] A. T. Le *et al.*, *J. Phys. B* **41** 081002 (2008).
  - [19] A. T. Le *et al.*, *Phys. Rev. Lett.* **102**, 203001 (2009).
  - [20] R. E. Stratmann and R. R. Lucchese, *J. Chem. Phys.* **102**, 8494 (1995).
  - [21] R. R. Lucchese *et al.*, *Phys. Rev. A* **25**, 2572 (1982).
  - [22] S. Ramakrishna and T. Seideman, *Phys. Rev. Lett.* **99**, 113901 (2007).
  - [23] O. Smirnova *et al.*, *Phys. Rev. Lett.* **102**, 063601 (2009).
  - [24] O. Smirnova *et al.*, *Nature* **460**, 972 (2009).
  - [25] M. Born and E. Wolf, *Principle of Optics* (Cambridge University Press, 1999).
  - [26] M. B. Gaarde, J. L. Tate, and K. J. Schafer, *J. Phys. B* **41**, 132001 (2008).
  - [27] C. Jin, A. T. Le, and C. D. Lin, *Phys. Rev. A* **79**, 053413 (2009).